

Design and Analysis of MEMS-based Microballoon Actuators for Aerodynamic Control of Flight Vehicles

A. Linga Murthy* and Y. Krishna**

*Research Center Imarat, Hyderabad-500 069

**Defence Research and Development Laboratory, Hyderabad

ABSTRACT

The development of microelectromechanical systems (MEMS) technology and the suitability and compatibility of sizes of microactuators with the boundary layer thickness fueled the active flow separation control to gain the air flow momentum for the last few years. The present paper deals with the development of a robust, large-deflection, and large-force MEMS-based microballoon actuator for aerodynamic control of flight vehicles such as projectiles, micro air vehicles, aircrafts, etc. Experiments were carried out on the scaled-up models for different input pressure conditions to study the response of microballoon actuator. To evaluate the performance of the microballoon actuators, simulation studies on MEMS scale models were conducted in the CoventorWare environment. Simulation studies involving static and dynamic analyses have been carried-out on the microballoon actuator models. Various geometric and input parameters influencing the behaviour of the microballoon actuator were investigated. It has been observed that a maximum deflection of 1.2 mm to 1.5 mm can be achieved using microballoon actuators and the maximum operational frequency of 60 Hz to 80 Hz can be used for the operation of microballoon actuators. Also, the sizes of the microballoon actuators designed are compatible and suitable to be used in turbulent boundary layer of aerodynamic flight vehicles.

Keywords: Microballoon actuators, MEMS, finite element analysis, dynamic behaviour, aerodynamic control

1. INTRODUCTION

The microelectromechanical systems (MEMS) technology enabled to design, model, and analyse the actuators and sensors of micro scale that are suitable for use within the boundary layer for flow separation control for developing ultra modern aerodynamic control systems with better efficiency and effectiveness. This type of microactuator-based active flow control is expected to greatly augment the conventional hinged type aerodynamic control systems for flight vehicles. Pneumatically-actuated microballoon actuator designed in the present work is fabricated using novel microfabrication technique with a silicon rubber MRTV-1 on robust silicon substrate as shown in Fig.1.

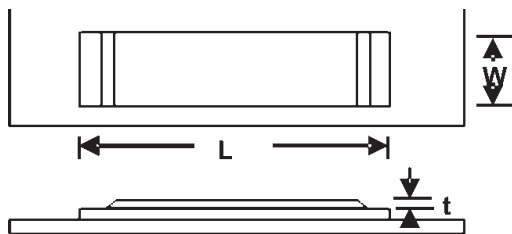


Figure 1. Schematic of microballoon actuator.

The dimensional and sectional details are shown in Fig. 2. Here, the diaphragm material used is silicon rubber MRTV-1, and the base material used is single crystal silicon/poly silicon. This microactuator has large deflection, low

power consumption, surface conformability and small size along the thickness of the wing. The boundary layer plays an important role in aerodynamic control of any flight vehicle. Coles and Hirst¹ presented a compilation of data on boundary layer subjected both to favorable

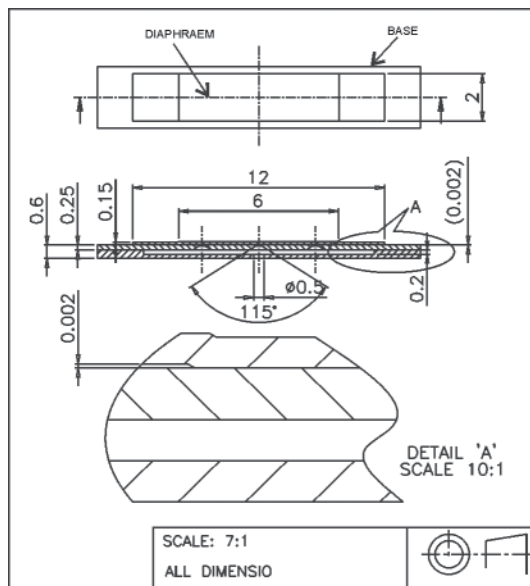


Figure 2. Dimensional and sectional view of pneumatically-actuated microballoon actuators.

and adverse pressure gradients and relaxing flow where pressure gradient were abruptly decreased and boundary layer relaxes to a new equilibrium. Spalart and Watmuff² have carried out experimental and numerical studies of boundary layers under varying pressure gradients. Hak³, described the flow issues in microactuators. The MEMS technologies offer the potential for the large-scale active control of coherent flow structures within the boundary layer, especially in a turbulent flow zone.

Warsop⁴ described the potential and status of MEMS for drag reduction and separation control stating that the future flying vehicles could benefit significantly from the application of aerodynamic flow control, which offers improvements in absolute performance (flying faster or slower, increased agility, reduced fuel burn) and the potential to reduce vehicle size, weight, and fuel consumption. The key mechanism for delaying flow separation is the addition of momentum to the near-wall region of the boundary layer. This can be achieved conventionally using brute force principles, which are generally inefficient and require high input energy levels with sufficient drag penalties. The present work tries to exploit the potential of MEMS technology to improve the efficiency of flow separation control as such systems would allow the energy input to the MEMS flow actuators to be minimised by maximising the use of natural instability mechanisms that occur within the boundary layer.

Deeds⁵ carried out investigations for viability of using MEMS to provide directional control of high speed projectiles. Tzong Shyng Leu⁶, *et al.* investigated the reduction of side force acting on a cone-cylinder slender body using a microballoon array actuator. The micro balloon array actuator can be inflated to a height of about 1.2 mm on the curve surfaces of slender body.

Grosjean⁷ first utilised the microballoon actuator for aerodynamic control. The maximum expansion of the actuator is approx 1.6 mm with 10 psi actuation pressure. They performed the aerodynamic experiments on fighter aircraft, F-15 using micro shear stress sensors and microballoon actuators packaged on the wing surface, as shown in Fig. 3.

Their experimental results indicated that the rolling moment could be effectively influenced once microballoon actuators were actuated at some positions. During operation it morphs the shape of the aerodynamic surface, creating

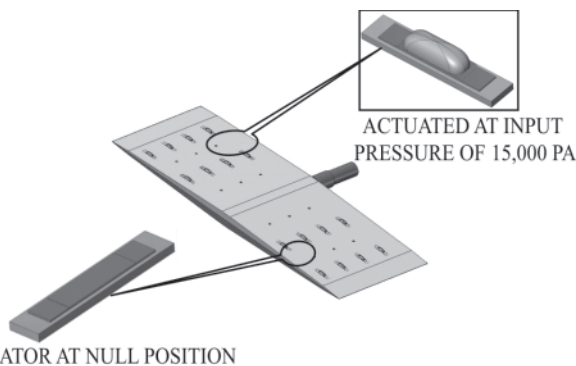


Figure 3. Microballoon actuators embedded in control surface.

a flow asymmetry, resulting in generation of side force to produce rolling, pitching or yawing moments for controlling the flight vehicle.

Literature survey reveals that large amount of work has been carried out in design, development, and production of microsensors, whereas in the case of microactuators, efforts for design, development, and production were relatively less. This could be due to the complexity of actuation system technology. The present work focuses on using microballoon actuators in turbulent boundary layer for flow separation control of aerodynamic flight vehicles.

2. DESIGN OF MICROBALLOON ACTUATOR

The design variables of the microballoon actuator include; base material, diaphragm material, shape of the diaphragm, length (L) width (W), thickness (t), and the input pressure (p). The base material selected was silicon due to its compatibility of microfabrication techniques. The microballoon actuator is modeled with base dimensions of $L= 6000 \mu\text{m}$, $W= 2000 \mu\text{m}$ and $t= 150 \mu\text{m}$. An extensive study carried out to identify the diaphragm material, silicon rubber MRTV-1 was chosen because of its high percentage of elongation and high tearing strength, which are the prime requirements for the functioning of a microballoon actuator. The rectangular shape diaphragm is selected to meet the aerodynamic requirements of the microballoon actuator. The properties of silicon rubber MRTV-1 are given in Table 1.

Table 1. Properties of silicon rubber MRTV-1

Tensile strength	: 3.5 MPa
Poisson's ratio	: 0.38
Young's modulus	: 0.9 MPa
Hardness	: 25 shore A
Service temp. range	: $-55 \text{ }^\circ\text{C}$ to $200 \text{ }^\circ\text{C}$

3. DESIGN OF EXPERIMENTAL MODELS OF MICROBALLOON ACTUATORS

The studies on the microballoon actuators require the translation of the MEMS scale models into experimental models. However, realising a MEMS scale microballoon actuators for experimental studies is prohibitively expensive and time-consuming due to the lack of adequate MEMS scale microfabrication facilities in the country. Hence, scaled-up experimental models (of scale 7:1)(Fig. 4) were designed using dimensional analysis and design of experiments (DOE) and used for the experimental studies to determine the functional relationship between the dependent variables, deflection and independent variables, input pressure, length, width, thickness, and material characteristics of the diaphragm of the microballoon actuators.

3.1 Dimensional Analysis

In the present work, experimentally obtained data from scaled-up models has been used to understand the behaviour of the MEMS scale conceptual model. The concept of similitude and dimensional analysis was used, so that the measurements made on the experimental models are applicable

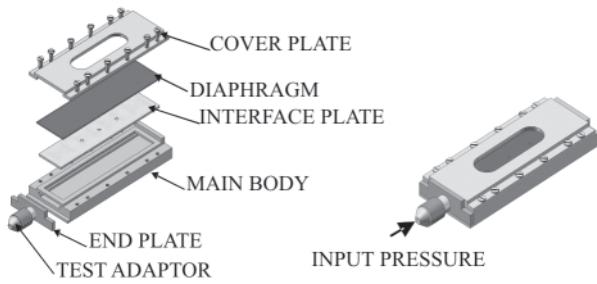


Figure 4. Scaled-up experimental model (scale 7:1).

to the MEMS scale models. Dimensional analysis was carried out to arrive at the model sizes for conducting the experimental studies on the model.

3.2 Design of Experiments

The experimentation involved four input (p , t , W and L) variables at three levels (low, medium, and high), and hence, the total number of experiments required would be $3^4=81$ (without replications). Considering the possible experimental errors, at least two replications would be needed. Thus, the total number of experiments needed would be $81 \times 3=243$. Since the variables involved in the experimentation included, length, width, and thickness of the diaphragm, the number of experimental models required would be very large. Keeping in view these problems, the DOE was used to minimise the number of experiments required. Various possible experimental designs were studied and 3^{k-p} and $4/1/27$ factorial design was selected with $k=4$ and $p=1$ and with four factors, one block, and 27 experiments. Two replications were considered with random sequence. The above design requires 27 types of experimental models and 81 experiments to be conducted in random sequence. The three levels of the input variables for scaled-up models (7:1 scale) are shown in Table 2.

Table 2. The three levels of input variables for scaled-up model (7:1 scale)

	Low	Medium	High
L (μm)	42000	49000	56000
W (μm)	14000	15400	16800
t (μm)	1050	1400	1750
p (Pa)	5000	10000	15000

4. EXPERIMENTAL STUDIES

4.1 Experimental Setup

The experimental setup involves; regulated pneumatic source, pneumatic control system, experimental models, and deflection measuring and recording systems. The experimental setup for measuring deflections of experimental models of the microballoon actuator is shown in Fig. 5.

4.2 Regulated Pneumatic Source

The regulated pneumatic source mainly consists of

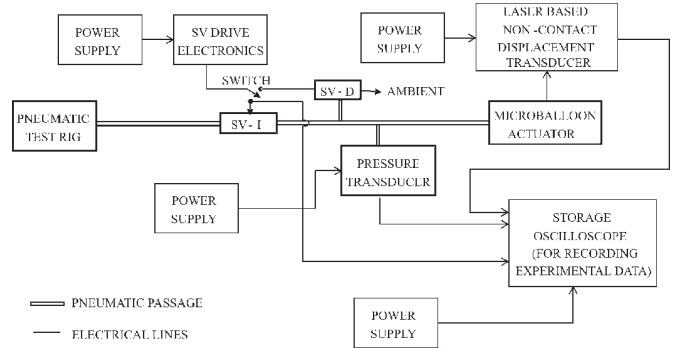


Figure 5. Experimental setup for measuring the deflection.

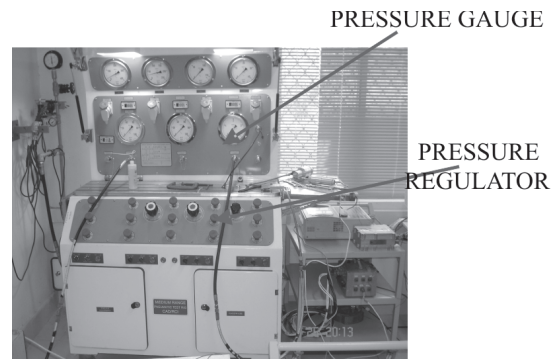


Figure 6. Pneumatic test rig with pressure regulators and indicators.

a pneumatic rig which receives air from the centralised air pressure supply system. The pneumatic rig houses the outlet pressure to the required constant pressure and pressure gauges/transducers to monitor the supplied pressure. Figure 6 shows the Pneumatic test rig with pressure regulators and indicators, needle valves for opening and closing the pneumatic supply, regulator for pressure regulation.

4.3 Pneumatic Pressure Control System

The pneumatic pressure control system mainly consists of two solenoid valves (one for inflation and the other for deflation of the microballoon actuators), a switching logic circuit (for driving the solenoid valves) and to on/off control of pressure to the microballoon actuators, and a pressure sensor (to provide the status of the microballoon actuators). Figure 7 shows the pneumatic pressure control system for conducting the experimental studies.

4.4 Measuring and Recording System

The deflection measuring and recording system shown in Fig. 8 consists of high accuracy ($< 10 \mu\text{m}$) laser-based non-contact type displacement transducer of Micro Epsilon make, and the high bandwidth (600 MHz) oscilloscope of Lecroy make (to record the deflections of the microballoon actuator). In each of the experiments, the steady-state deflection of the microballoon actuator were measured and recorded using measuring and recording system.

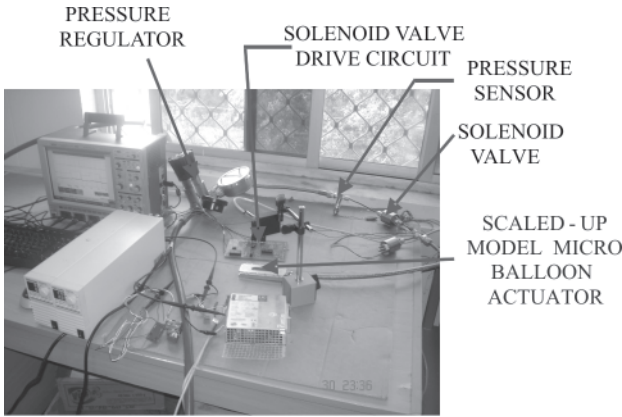
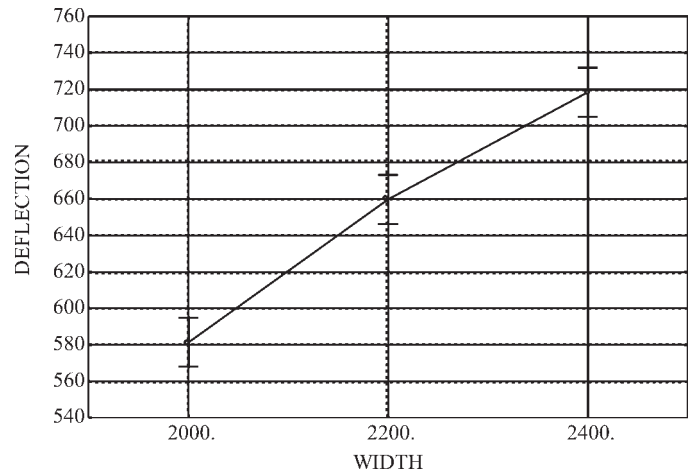


Figure 7. Pneumatic pressure control system.



(b)

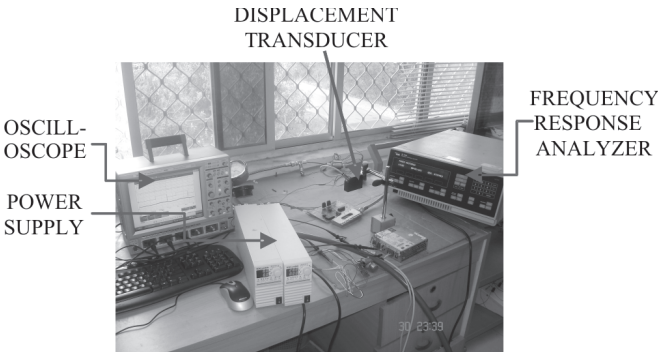
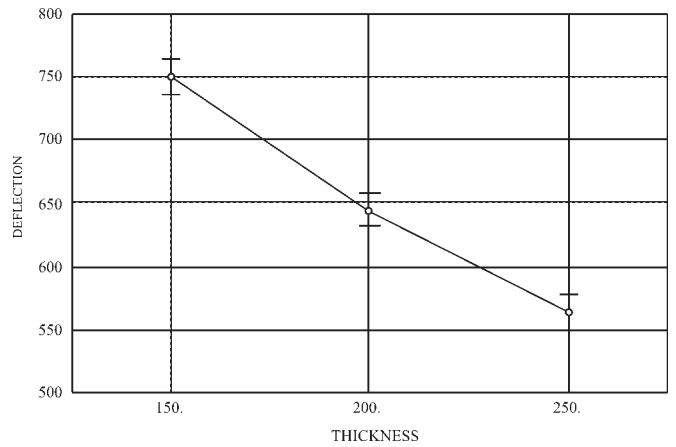


Figure 8. Deflection measuring and recording system used in the experimental studies.



(c)

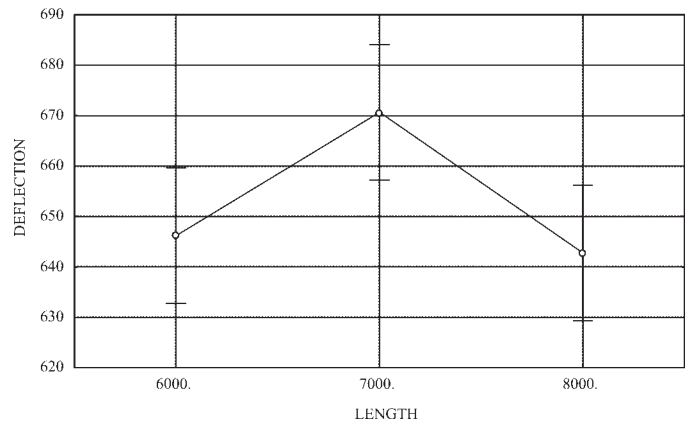
5. EXPERIMENTAL RESULTS

The experimental results obtained in terms of deflections were converted in to the range of MEMS scale model deflections (μm) by dividing a scale factor of 7 according to the modelling laws of dimensional analysis.

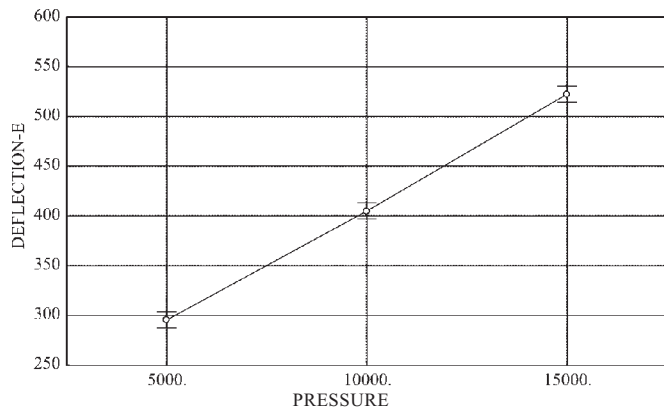
The effects of p , t , W , and L on deflections are shown in Figs 9 (a) to 9(d) and two-way and three-way interaction effects are shown in Figs 10 and 11, respectively.

The experimental results indicate the following:

- The influence of the diaphragm length on the deflection was found to be very low as compared with the other parameters.



(d)



(a)

Figure 9. Main effects of p , t , W & L on deflection. Plot of marginal means and conf. limits (95.%) DV: deflection-E design: 4 3-level factors, 1 blocks, 81 runs. (Note: Std. Errs. for means computed from MS Error=1230.454)

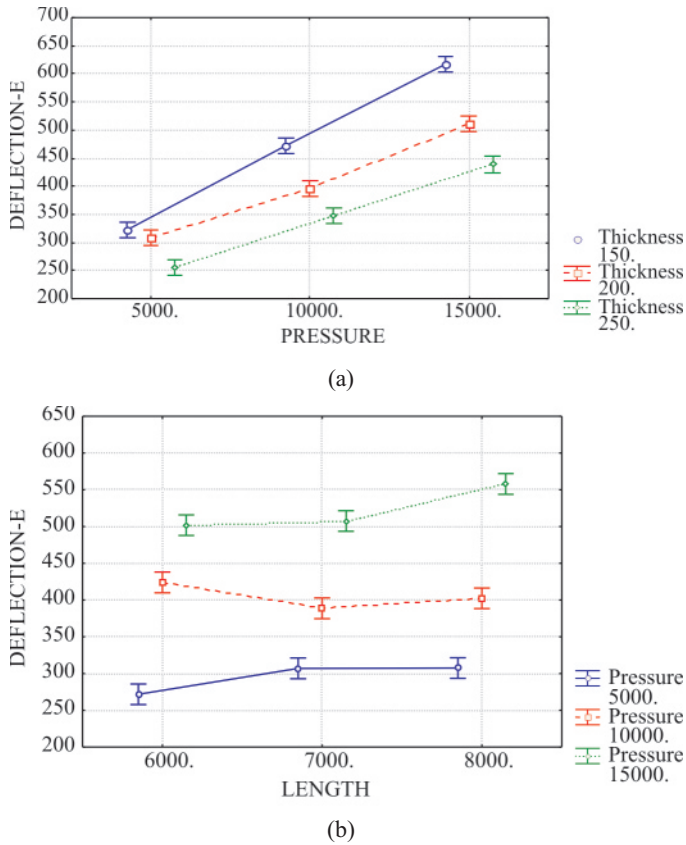


Figure 10. Two-way interaction effects of (a) p and t (b) p and L on model ($f1$) Plot of marginal means and Conf. limits (95.%) DV: deflection-E design: 4 3-level factors, 1 blocks, 81 runs. (Note: Std. Errs. for means computed from MS error=440.4677)

- The width of the diaphragm has a positive influence on the deflection. As the width increases, the deflection increases linearly. The influence of the diaphragm width appears to be more than the length, but less than the thickness. This result could be due to the rectangular shape of the microactuator with the length-to-width ratio >2 . The width, which is smaller, would be the limiting factor for deflection.
- The thickness of the diaphragm appears to have maximum influence on the deflection of the actuator. The thickness of the diaphragm has a negative influence on the deflection of the microballoon actuator, and it is evident, as the expansion of the balloon is always an inverse function of its thickness. The deflection decreases linearly with increasing thickness of the diaphragm.
- The input pressure has a positive influence on the deflection of the microballoon actuator. This is an obvious result.
- Maximum deflection was 750 μm at pressure of 15000 Pa.

6. DESIGN AND SIMULATION OF MEMS SCALE MODELS

CoventorWare environment has been used to develop the simulation models of the microballoon actuators to

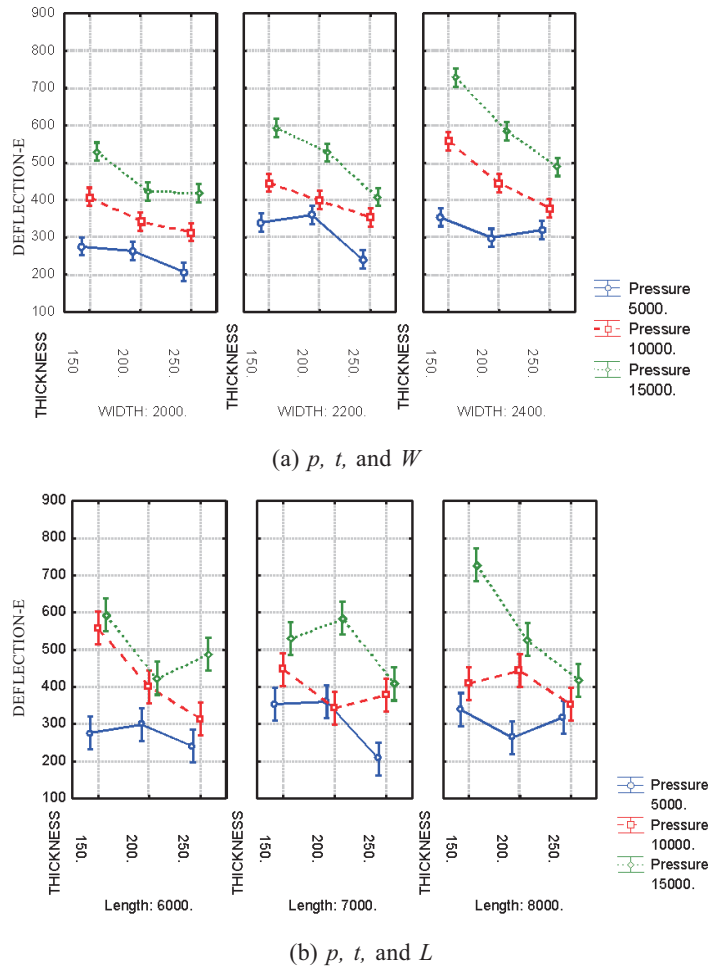


Figure 11. Three-way interaction effects of (a) p , t and W (b) p , t and L on model1 ($f1$) plot of marginal means and conf. limits (95.%) DV: deflection-E design: 4 3-level factors, 1 blocks, 81 runs. (Note: Std. Errs. for means computed from MS Error=440.4677)

study the steady state and dynamic behaviour. This environment is MEMS specific design and simulation tool. The simulation studies carried out included:

- Steady-state analysis, for deflection and stress, modal analysis and harmonic analysis.
- The deflections obtained in simulation and experiments were correlated.
- The correlation coefficient was found to be 0.972603, which is > 0.95 , and hence, the model is validated. The correlation of deflections obtained in simulation and experimentation are shown in Fig. 12.

7. STRESS (STATIC) ANALYSIS

The stress analysis was carried out using CoventorWare software on diaphragm of the microballoon actuator for the diaphragm dimensions of extreme case of 8000 (L) X 2400 (W) X 150 (t) at an input pressure of 30,000 Pa. The details of stress analysis are shown in Fig. 13.

7.1 Results and Discussions of system analysis

The results of the stress analysis indicate that the

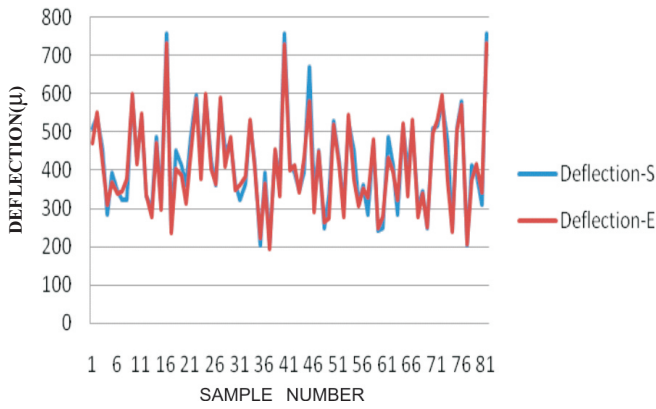
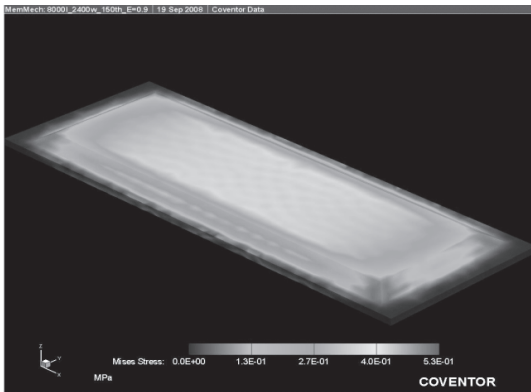
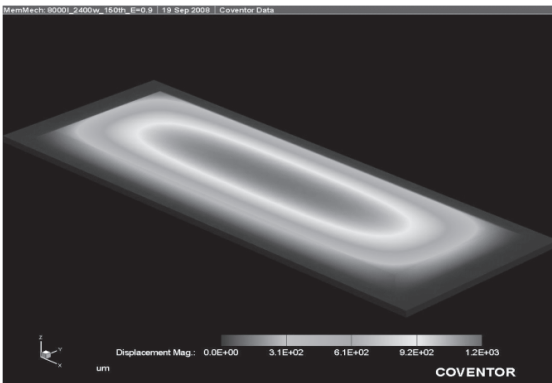


Figure 12. Correlation of experimental and simulation results.



(a) STRESS PLOT



(b) DISPLACEMENT PLOT

Figure 13. Stress and displacement plots of 8000 (*L*) × 2400 (*W*) × 150 (*t*).

maximum stress experienced by the diaphragm is of the order of 0.53 MPa; the maximum deflection was found to be about 1.2 mm; the location of the maximum stress is found to be at the edges; and the factor of safety is >4.

8. MODAL ANALYSIS

Modal (resonant frequency) analysis was conducted to study the dynamic behaviour of the microballoon actuator. The prime objective of the study was to determine the modal or resonant frequencies of the microballoon actuator

at different design conditions and input pressures. In this analysis the effect of variation of the input $L = 6000$ to $8000 \mu\text{m}$ with step size of $1000 \mu\text{m}$ $W = 2000$ to $2400 \mu\text{m}$ with step size of $200 \mu\text{m}$ $t = 150$ to $250 \mu\text{m}$ with step size of $50 \mu\text{m}$ $p = 5000$ to 15000 Pa with step size of 5000 Pa

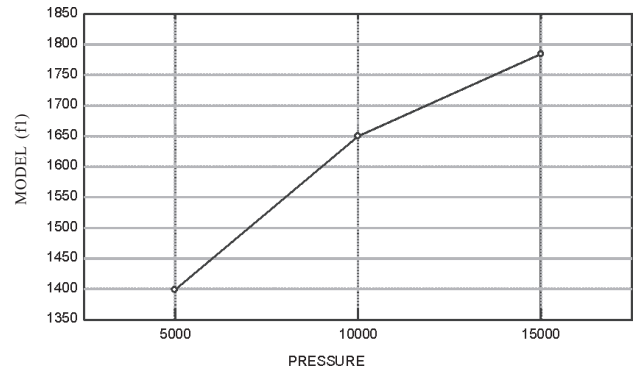
The simulation results of modal analysis were extracted for the first five modal (bending mode shapes) frequencies. Since the first modal frequency (mode 1 (*f*1)) is considered to be dominant from the practical point of view, the simulation results for this frequency were analysed using analysis of variance (ANOVA). The results of ANOVA are presented.

The behavior of the first modal frequency (mode1 (*f*1)) with the variation of pressure, thickness, width, and length of the diaphragm of the microballoon actuator is presented in Figs 14 to 16.

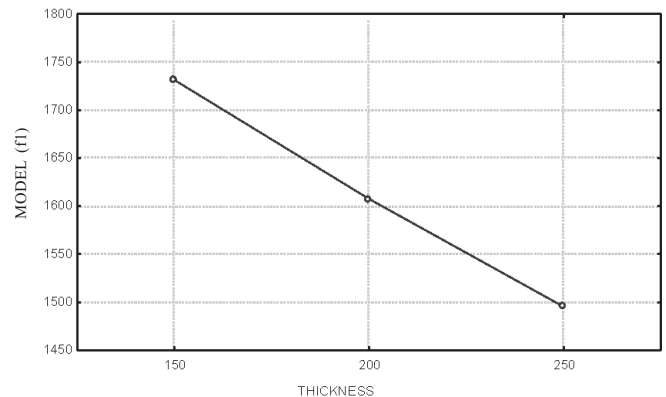
8.1 Results and Discussions of Modal Analysis

The results of the modal analysis are:

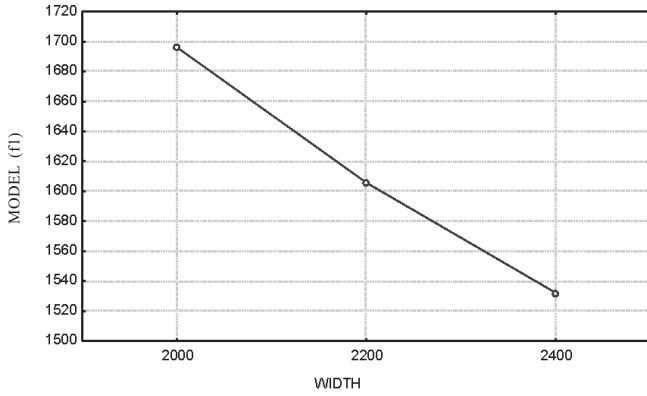
- The input pressure has the positive influence on modal frequency (*f*1). This result is obvious due to fact that the effective stiffness increases with increase of pressure.
- The width and length of the diaphragm have the negative influence on *f*1 and they have inverse relation with modal frequency (*f*1). This happens because of the fact that the stiffness decreases with increase of width and length.



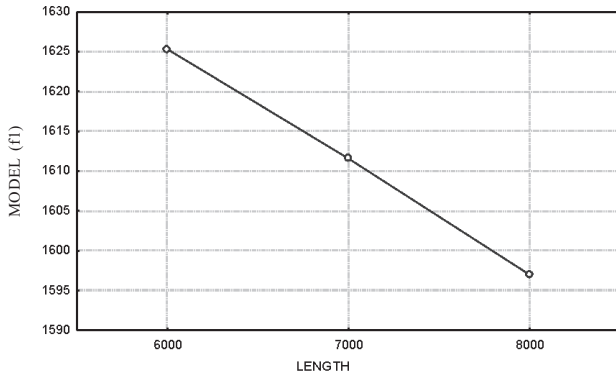
(a)



(b)

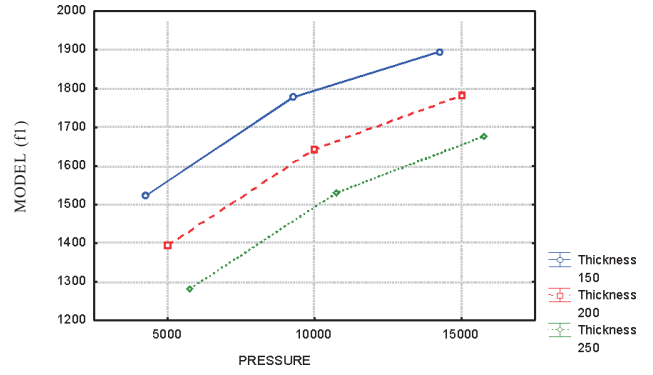


(c)

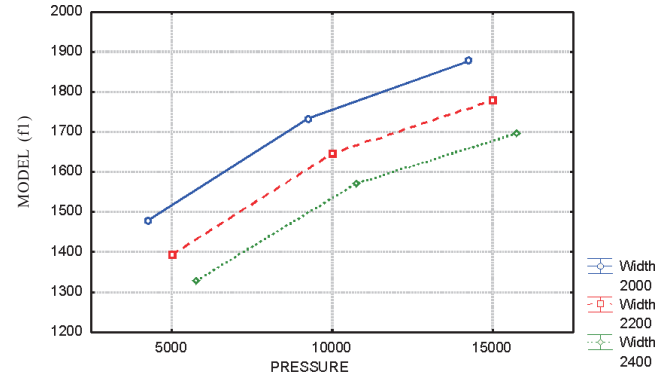


(d)

Figure 14. Main effect of: (a) Pressure, (b) thickness, (c) width, and (d) length on modal frequency model1 ($f1$). (Unweighted means, current effect: $F(2, 0)$ ---, $p=$ ---, effective hypothesis decomposition, vertical bars denote 0.95 confidence intervals)

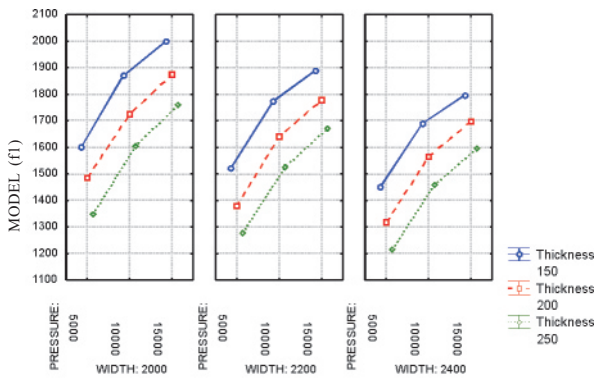


(a)

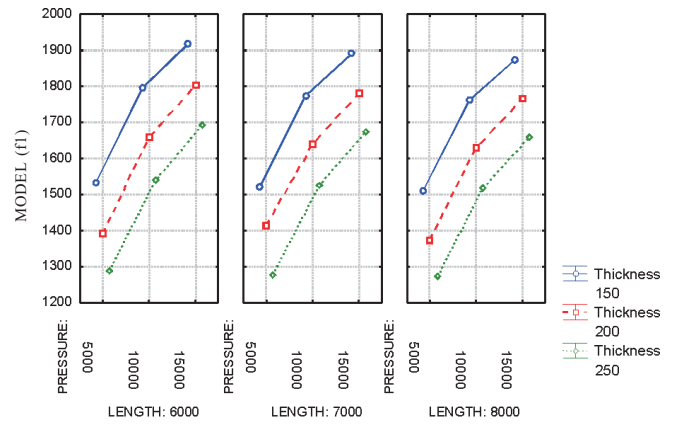


(b)

Figure 15. Two-way interaction effects of : (a) p and t , and (b) p and W on model ($f1$). (Unweighted means, current effect: $F(4, 0)$ ---, $p=$ ---, effective hypothesis decomposition, vertical bars denote 0.95 confidence intervals)



(a) p , t , and W



(b) p , t , and L

Figure 16. Three-way interaction effects of: (a) p , t and W and (b) p , t and L on model ($f1$). (Pressure * Thickness* Length; unweighted means , current effect: $F(8, 0)$ ---, $p=$ --- effective hypothesis decomposition, vertical bars denote 0.95 confidence intervals)

- In the case of thickness of the diaphragm, it has the negative influence and inverse effect on $f1$. As the thickness of the diaphragm increases both mass and stiffness of the diaphragm increase. The reduction of modal frequency appears to be due to fact that the effect of mass is more than the stiffness.
- From the results shown in the graphs, it appears that the two-way and three-way interaction effects are almost negligible.
- The modal frequency ($f1$) was found to be between 1200 Hz to 2100 Hz for the specified range of dimensions of the diaphragm and input pressure given in para⁶.

9. MODAL HARMONIC ANALYSIS

The modal harmonic analysis studies were carried out on the diaphragm of the actuator for the diaphragm dimensions for input pressure of 30000 Pa. The displacement amplitude and phase characteristics obtained in the studies are presented in Fig. 17.

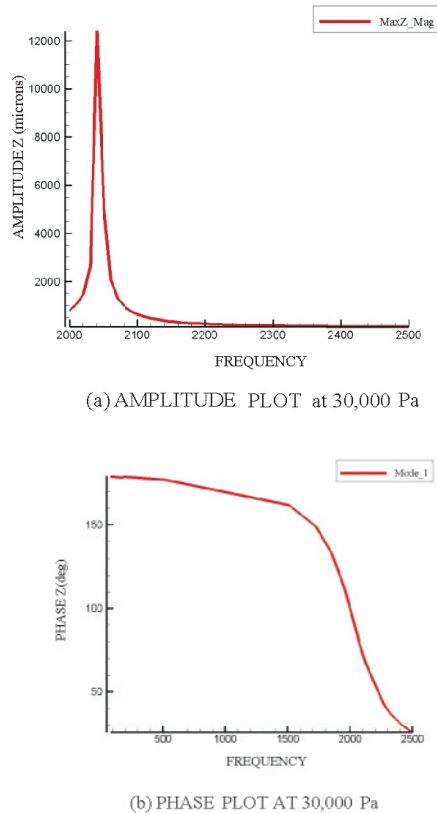


Figure 17. Modal harmonic analysis results for 6000(L), 2000(W) and 150 thickness.

10. CONCLUSIONS

Following are the conclusions drawn:

- The deflections of about 750 μm are obtained at the input pressure of 15,000 Pa (0.15 bar).
- The maximum stress induced in the diaphragm of the actuator was 0.53 MPa at an input pressure of 30,000 Pa and the factor of safety is found to be > 4 .
- The modal frequencies for the first five modes were found to be between 1200 Hz to 2400 Hz for the given range of dimensions of the diaphragm for the input pressures up to 15,000 Pa.
- A high amplitude peak was found at first modal frequency indicating the resonance effect.

The outcome of this research work is useful for designing the flight vehicles such as projectiles, MAVs, UAVs, etc., with enhanced aerodynamic effectiveness and man-euvering capabilities.

This work extends the previous research work Leu⁶ and Grosjean⁷ from the perspective of control force generation for certain defence applications in India.

REFERENCES

1. Coles, D. & Hirst, A.E. Computation of turbulent boundary layers. In AFOSR-IFP Stanford Conference, CA, 1969.
2. Spalart, P.R. & Watmuff, J.H. Experimental and numerical study of a turbulent boundary layer with pressure gradient. *J. Fluid Mech.*, 1993, **249**, 337-71.
3. Gad-el-Hak, Mohamed. The fluid mechanics of microdevices-the freeman scholar lecture. *ASME*, 1999, **121**(5).
4. Warsop, Clyde. MEMS and microsystems technologies their potential and status for drag reduction and separation control. In European Congress on Computational Methods in Applied Sciences and Engineering, 2004.
5. Deeds, Michael. Development and testing of MEMS control surfaces for high speed projectiles. In 45th AIAA Aerospace Sciences Meeting and Exhibit, Reno, Nevada, 8-11 January 2007. pp.1-14.
6. Leu, Tzong-Shyng. Side force reduction of cone-cylinder using microballoon array actuator. *J. Prop. Power*, 2005, **2**.
7. Grosjean, C. Microballoon actuators for aerodynamic control. In IEEE Microelectromechanical Systems Workshop (MEMS'98), Heidelberg, Germany, 1998.

Contributors



Mr A. Linga Murthy obtained his ME and is perusing PhD (Mechanical Eng.) from Osmania University, Hyderabad. He is working as a Scientist at the Research Centre Imarat, Hyderabad. He is engaged in design and development of control actuation systems and microelectromechanical systems (MEMS)

devices for flight vehicles. His areas of interest include: Microactuators, smart actuators, wireless sensors, and actuators. He has published many papers in national and international conferences.



Dr Y. Krishna obtained his PhD (Mechanical Engg) from the Indian Institute of a Science, Bengaluru. Presently, he is working as Scientist at the Defence Research Development Laboratory, Hyderabad. He is actively engaged in the design, analysis, and testing of airframes and structural components of various missiles. His

areas of interest include: Structural dynamics, active vibration control, FEM, and related areas. He has published many papers in national and international conferences.